with water/glycerol mixtures of known viscosity.

The results obtained are shown in Fig. 2, with viscosity plotted on a logarithmic scale against the reciprocal of absolute temperature. The absolute accuracy is ± 10%. The $BaO:B_2O_3$ flux (60:40) has a viscosity of 0.6 P at 1050°C. The addition of 15% by weight of YIG dramatically increases this to 1.9 P. Although BaF_2 addition decreases the viscosity, the effect is not substantial. The results should be compared with those for a typical growth solution using the $PbO—B_2O_3$ flux, which has a viscosity of 7×10^{-2} P at 1050°C [12]. Since the flux consisting of $BaO:BaF_2:B_2O_3$ in a molar ratio of 30:50:20 had the lowest viscosity, this composition was used for epitaxial growth but even so the adhesion of melt droplets to the epilayer surface was still apparent.

Although $BaO—B_2O_3$ fluxes have a number of desirable features for the epitaxial growth of garnet, their high viscosity makes the removal of residual melt from the epilayer surface extremely difficult. Unless more effective ways of removing this excess melt can be devised, the use of the $BaO—B_2O_3$ flux for garnet epitaxy is severely limited.

Acknowledgements

The authors would like to thank Mr J. D. C. Wood for useful discussions, and the Science Research Council for financial support.

References

1. H. J. LEVINSTEIN, S. LICHT, R. W. LANDORF and S. L. BLANK, *Appl. Phys. Letters* **19** (1971) 486.
2. E. A. GIESS, J. D. KUPTSIS and E. A. D. WHITE, *J. Crystal Growth* **16** (1972) 36.
3. E. A. GIESS, D. C. CRONEMEYER, R. GHEZ, E. KLOKHOLM and J. D. KUPTSIS, *J. Amer. Ceram. Soc.* **56** (1973) 593.
4. R. C. LINARES, *ibid* **45** (7) (1962) 307.
5. R. HISKES and R. A. BURMEISTER, in "Magnetism and Magnetic Materials" (edited by C. D. Graham, Jun and J. J. Rhyne) No. 10 (1973) 304.
6. E. M. LEVIN and H. J. MCMURDIE, *J. Res. Nat. Bur. Stand.* **42** (1949) 135.
7. R. GHEZ and E. A. GIESS, *Mat. Res. Bull.* **8** (1973) 31.
8. J. A. BURTON, R. C. PRIM and W. P. SLICHTER, *J. Chem. Phys.* **21** (1953) 1987.
9. C. M. LAWRENCE, P. CAPPER, I. M. COE and D. ELWELL, BACG Conference on Crystal Growth, York (1973).
10. H. R. LILLIE, *J. Amer. Ceram. Soc.* **12** (1929) 505.
11. M. MARGULES, *Sitz. Ber. Akad. Wiss. Wien.* **83** (1881) 588.
12. J. E. DAVIES, E. A. D. WHITE and J. D. C. WOOD, *J. Crystal Growth*, to be published.

Received 22 February
and accepted 4 March 1974

J. E. DAVIES*
E. A. D. WHITE
Department of Electrical Engineering,
Imperial College of Science and Technology,
London, UK

---

*Present address: IBM, T. J. Watson Research Center, Yorktown Heights, New York, 10593, USA.

Fibre diameter measurement by laser diffraction

One problem involved in studying the tensile properties of fine fibres is determining the effective cross-section. For smooth, parallel-sided fibres of circular section the problem reduces to one of diameter determination; the diameters involved for carbon fibres, for example, are of the order 7 to 10 μm. Two methods have been employed to date: firstly, the use of a pre-calibrated image shearing eye-piece on an optical microscope for direct measurement [1, 2], and secondly, the interpretation of the diffraction pattern from an incident laser beam [3, 4] – this latter being illustrated in Fig. 1. Both methods allow a rapid determination of the required diameter.

A comparison between diameters as determined both by laser diffraction and on an optical projection microscope showed [4] the existence of a difference of the order of $\frac{1}{3}$ μm with the laser value being the smaller. Whilst the difference was not significant in that work [4], this article reports a preliminary study to understand the origin of the difference.

The simplest interpretation of the laser diffraction pattern of a fibre can be understood as follows. The pattern created by an infinitely thin lath of width d_S is the same as that of a slit of the same width. It is a series of maxima and minima on either side of a central maximum as indicated in Fig. 1. The separation δ_S between the first corresponding pair of minima is given in the Fraunhofer approximation by the relation

$$\delta_S = \frac{2\lambda_S}{d_S} \qquad (1)$$

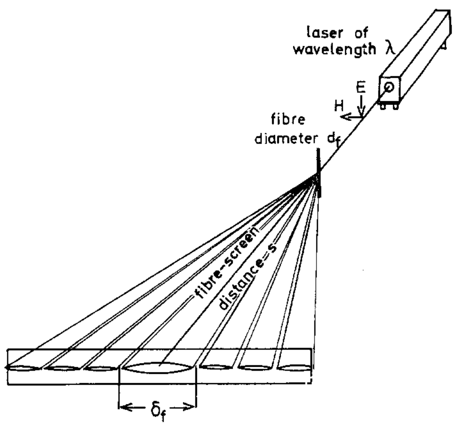

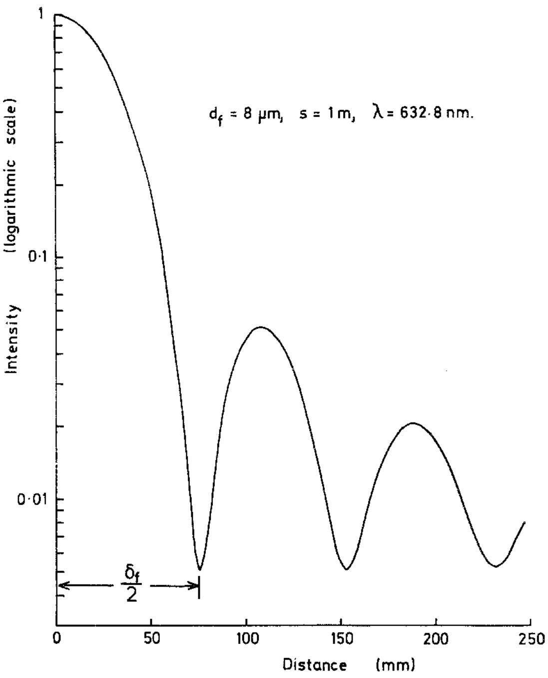

Figure 1 The diffraction of a laser beam in TM mode by a fine fibre. Also indicated is the calculated intensity profile for an 8 μm diameter fibre at a distance of 1 m using a He–Ne laser of 632.8 nm wavelength.

where s is the screen-lath distance and λ is the laser wavelength. If it is assumed that a fibre diffracts like a slit (the slit approximation) then its diameter can immediately be derived from Equation 1. This was done in an earlier study [4].

The diffraction pattern of a real fibre can be calculated [5] but requires knowledge of the refractive index m of the fibre. In the case of a perfectly reflecting fibre ($m = \infty$) of diameter d_f the scattered intensity is given by [5]:

$$\frac{I_{\text{TM}}}{I_0} = \frac{2}{K_0 s \,.\, \pi} |b_0 + 2 \sum_{n=1}^{\infty} b_n \cos(n\theta)|^2 \cdot \qquad (2)$$

The incident intensity I_0 is polarized along the axis of the fibre (TM mode). Its direction of propagation is perpendicular to the fibre axis, θ is the scattering angle and $K_0 = 2\pi/\lambda$. The constants b_n are given by [5]:

$$b_n = J_n(\alpha)/H_n^{(2)}(\alpha) \qquad (3)$$

where $\alpha = \pi d_f/\lambda$; $J_n(\alpha)$ and $H_n^{(2)}(\alpha)$ are Bessel functions and second Hankel functions respectively.

We have evaluated the diffraction pattern for a range of values of α; a specific case is included in Fig. 1. The locations of the minima are different from those calculated for a slit. Calling the distance between the first pair of minima δ_f, then the relative difference from the slit case, $(\delta_s - \delta_f)/\delta_s$, is given in Fig. 2 as a function of α.

Experiments have been carried out to compare the diffraction pattern minima of fibres of known diameters with the diffraction pattern minima calculated for a slit (Equation 1) of the same width for a range of values of α_f. A set of four tungsten wires (kindly made available by Mr W. Watt of R.A.E. Farnborough) duly calibrated with an image shearing eye-piece were used in association with an Argon laser and a He–Ne laser. A total of four wavelengths were used. The diffraction pattern was measured on a graduated transluscent screen set perpendicular to the laser beam at a distance s of 1 m from the fibre. The distance between the measured separation of the first pair of minima δ_f and that calculated for a slit δ_s of the same width (i.e.

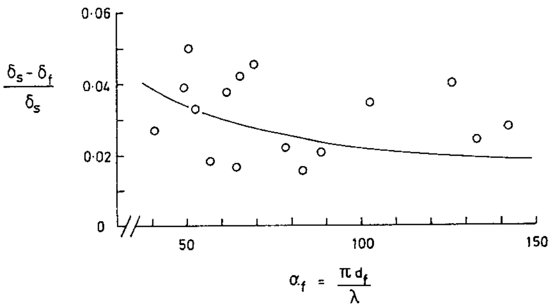

Figure 2 The difference between the separation of the first pair of minima δ_f calculated for a perfectly reflecting ($m = \infty$) fibre of diameter d_f and the calculated separation δ_s for a slit of the same width relative to δ_s as a function of α. Superimposed are experimental data for fibre diameters of 8.1, 10.1, 12.9 and 20.7 μm and wavelengths of 457.9, 488.0, 514.5 and 632.8 nm.

$d_s = d_f$) relative to δ_s are superimposed on the curve in Fig. 2. The agreement is quite reasonable although it should be born in mind that the tungsten fibres are not perfectly reflecting. It is not anticipated, however, that some degree of absorption is likely to be significant.

Fig. 2 can also be used to determine the diameter of a real fibre. From Equation 1 we see that $\alpha_s = 2\pi s/\delta_s$. As $\delta_s \cong \delta_f$ and $d_s \approx d_f$ we get a good estimate of the parameter α in Fig. 2 by putting $\alpha = 2\pi s/\delta_f$. A corrected value for the real diameter d_f from the measured quantity δ_f is thus given by

$$d_f \cong 2\lambda \,.\, s/\delta_f \left[1 + \left(\frac{\delta_s - \delta_f}{\delta_s}\right)_{\text{corr}}\right]$$

where $[(\delta_f - \delta_s)/\delta_s]_{\text{corr}}$ was taken from Fig. 2. The relative error in the determination of d_f is now of the order of $[(\delta_f - \delta_s)/\delta_s]^2_{\text{corr}}$.

We conclude that the diffraction pattern of a real fibre is sufficiently different from that of a slit to warrant the slit approximation being treated with caution. In principle, the laser diffraction method, as discussed here, is capable of high precision for diameter measurements. Another case where the difference is also significant occurs where one compares the diffraction pattern of a slit with that of a fibre as discussed elsewhere [6].

References

1. W. WATT, L. N. PHILLIPS and W. JOHNSON, *The Engineer* (May 27) (1966) 815.
2. R. MORETON, *Fibre Sci. Tech.* **1** (1969) 273.
3. M. KOEDAM, *Philips Tech. Rund.* **27** (1966) 182.
4. A. J. PERRY, K. PHILLIPS and E. DE LAMOTTE, *Fibre Sci. Tech.* **3** (1971) 317.
5. M. KERKER, "The Scattering of Light" (Academic Press, New York, 1969) p. 255.
6. R. DÄNDLIKER and B. INEICHEN, *ZAMP* **23** (1972) 163.

Received 11 March
and accepted 3 April 1974

A. J. PERRY
B. INEICHEN
B. ELIASSON
Brown Boveri Research Center,
CH-5401 Baden,
Switzerland

Vapour transport of aluminium into fluxed melts, via reaction of PbF_2 with sillimanite

PbF_2 has been shown to react with sillimanite, Al_2SiO_5, producing a gaseous siliceous species which diffuses into fluxed melts and leads to the growth of silicate crystals by a "vapour-flux" process [1]. Since aluminium is also transported by PbF_2 [2], and since crystals of $ZnAl_2O_4$ and $BaO \,.\, 6Al_2O_3$ have been grown above melts containing their components and PbF_2 [3], it seemed probable that the latter would react with sillimanite, transporting aluminium. This note describes the growth of aluminates and aluminosilicates by the "vapour-flux" process.

The chemicals used, and their content of Si and Al, are shown in Table I. The starting materials were contained in platinum crucibles of 10 cm³ capacity, with loosely-fitting lids. The crucibles, in batches of 4 or 6, were placed on slabs of Morgan M.I. 3000 refractory brick in a D-shaped sillimanite muffle which was 27 × 11 cm² in base area × 8 cm in height and closed at one end. The muffle was situated in a furnace and the open end blocked by a plug of refractory brick.

The starting compositions, experimental conditions and crystals obtained are shown in Table II. Details of the identification of the crystals by EPMA and X-ray powder patterns are given in Table III.

$MgAl_2O_4$. Transparent octahedra were found in a platinum crucible, which contained initially only high purity MgO and PbF_2, after the PbF_2 had evaporated in the muffle. The X-ray powder pattern of the crystals corresponded closely to that of $MgAl_2O_4$ [4], and the identification was confirmed by EPMA. $Mg_2SiO_4 . MgF_2$ crystallized also from the same melt [1]. This result contrasts with many experiments with identical materials carried out in an open furnace or a platinum tube; here only MgO crystals were obtained.

Dy_2SiO_5, $DyAlO_3$, $Dy_3Al_5O_{12}$ and other aluminates. Three distinct phases grew in a melt

TABLE I Concentration of Al and Si in the chemicals (ppm)

	Al	Si
Rare Earth Products 99.9% R_2O_3	approx. 5	approx. 40
"Specpure" MgO	1	1
BDH "Optran" PbF_2	15	2
BDH "Analar" PbO	3	2
BDH "Analar" PbO_2	13	90
BDH "Analar" MoO_3	270	1000
BDH Lab. Reagent SiO_2	3000	